

Zeolite powder based polyurethane sponges as biocarriers in moving bed biofilm reactor for improving nitrogen removal of municipal wastewater

Zi Song^{1,2}, Xinbo Zhang^{1,2,*}, Huu Hao Ngo^{1,4,*}, Wenshan Guo^{1,4}, Pengfei Song³, Yongchao Zhang^{1,2}, Haitao Wen^{1,2}, Jianbo Guo^{1,2}

¹ *Joint Research Centre for Protective Infrastructure Technology and Environmental Green Bioprocess, School of Environmental and Municipal Engineering, Tianjin Chengjian University, Tianjin 300384 and School of Civil and Environmental Engineering, University of Technology Sydney, NSW 2007, Australia*

² *Tianjin Key Laboratory of Aquatic Science and Technology, Tianjin Chengjian University, Jinjing Road 26, Tianjin 300384, China*

³ *School of Environmental and Municipal Engineering, Xi'an University of Architecture and Technology, Xi'an 710055, China*

⁴ *Centre for Technology in Water and Wastewater, School of Civil and Environmental Engineering, University of Technology Sydney, Sydney, NSW 2007, Australia*

* *Correspondence author. Email address: ngohuuhao121@gmail.com and Xinbo Zhang, Email address: zxbcj2006@126.com*

Abstract

This study aims to enhance nitrogen removal efficiency of a moving bed biofilm reactor (MBBR) by developing a new MBBR with zeolite powder-based polyurethane sponges as biocarriers (Z-MBBR). Results indicated the total nitrogen (TN) removal efficiency and simultaneous nitrification and denitrification (SND) performance in Z-MBBR were nearly 10% higher than those in the conventional MBBR with sponges as biocarriers (S-MBBR). About $84.2 \pm 4.8\%$ of TN was removed in Z-MBBR compared to $75.1 \pm 6.8\%$ in S-MBBR. Correspondingly, the SND performance in Z-MBBR and S-MBBR was $90.7 \pm 4.1\%$ and $81.7 \pm 6.5\%$, respectively. The amount of biofilm attached to new biocarriers ($0.470 \pm 0.131\text{g/g}$ carrier) was 1.3 times more than that of sponge carriers ($0.355 \pm 0.099\text{g/g}$ carrier). Based on the microelectrode measurements and microbial communities analysis, more denitrifying bacteria existed in the Z-MBBR system, and this can improve the SND performance. Consequently, this new Z-MBBR can be a promising option for a hybrid treatment system to better nitrogen removal from wastewater.

Keywords: modification of polyurethane sponge; bioreactor; simultaneous nitrification and denitrification (SND); microelectrode; microbial community

1. Introduction

As the eutrophication of water bodies is a serious environmental concern removing nitrogen from wastewater has become a major priority in the field of water pollution control (Chu and Wang, 2011; Gao et al., 2018). Due to the large amount of sludge discharge and the short sludge age in the activated sludge process, meeting the requirements of high efficiency nitrification is difficult to achieve. Therefore, biofilm technologies are increasingly being implemented in wastewater treatment, and these include the following: trickling filter, rotating contactor, biological contact oxidation process, moving bed biofilm reactor, and biological aerated filter (Sbardella et al., 2018; Walser et al., 2016; Zhang et al., 2017). Amongst the above, the MBBR process has proved to be a simple yet effective and compact technology for wastewater treatment where microorganisms grow as a biofilm on the surfaces of suspended carriers (Bakar et al., 2018; Odegaard and Rusten, 1994; Shi et al., 2017).

One of the key elements of MBBR is the biofilm carriers, where properties such as material, surface roughness and specific surface area are considered. They can directly affect the speed of biofilm and the amount of microorganisms, and this results in the MBBR treating wastewater efficiently (Abzazou et al., 2016; Chu et al., 2014). To date, various biocarriers have been introduced in the MBBR process, including plastic media, polyurethane sponge, activated carbon, natural occurring materials, non-woven carriers, ceramic carriers, and modified carriers (Deng et al., 2016; Peng et al., 2018; Young et al., 2016). Of all the above, polyurethane sponge can be considered as an ideal growth medium for its high mechanical strength, large specific surface area, rough surface and good adhesion to microorganisms (Luo et al., 2014). Another advantage of polyurethane sponge is that it has advanced simultaneous

nitrification and denitrification (SND) properties due to the highly dissolved oxygen (DO) gradient in the cubic biofilm (Zhang et al., 2016).

Despite these advantages, scholars anticipate finding new ways to improve the performance of polyurethane sponge, such as modification (hydrophilic or charged modification) or in combination with other carriers. Chu et al.(2014) investigated the hydrophilic cationic modified polyurethane foam (MPUF) carriers. Their results revealed that the amount of biofilm attached to MPUF carriers was 1.3 times more than that attached to polyurethane foam (PUF) carriers at the steady state of reactor operation. Furthermore the effluent ammonium concentration was lower than 5.0 mg/L and a removal efficiency of 77–91% was achieved. The conventional high-density polyethylene (HDPE) carriers were modified by two kinds of positively charged polymers with different charge strengths as reported by Mao et al. (2017). Consequently, the average value of TN removal efficiency with modified PQAS-10 carriers was 72%, and higher than this was modified CPAM carriers (63%), and unmodified HDPE carriers (49%). Deng et al. (2016) used the electrophilic suspended biofilm carriers for MBBR, and the MBBR with sponge modified biocarriers (S-MBBR) produced better effluent quality and enhanced nutrient removal at HRTs of 12 h and 6 h compared to the MBBR with plastic carriers. However, many studies on the modification of biocarriers have introduced other chemicals, which are not economical and environmentally friendly. So far, no one has combined zeolite powders with polyurethane sponge as a biofilm carrier as a physical method approach. Since zeolite has large porosity and a large specific surface area (Sancho et al., 2017), as a biofilm carrier it exhibits good adsorption performance, and subsequently has been widely used in the field of wastewater

treatment.

The purpose of this investigation is to enhance nitrogen removal efficiency of a moving bed biofilm reactor (MBBR) by developing a new MBBR with zeolite powder-based polyurethane sponges as biocarriers (Z-MBBR). The performance of MBBR was evaluated in terms of: (1) nitrogen removals; (2) simultaneous nitrification and denitrification performance; (3) the DO and ORP profiles within the biocarriers of both reactors by microelectrode measurements; (4) the differences between the S-MBBR and Z-MBBR regarding biodiversity, microbial community evolution and the functional bacteria on nitrogen removal; and (5) the feasibility of the Z-MBBR becoming part of a hybrid MBBR-MBR system to improve the TN removal efficiency .

2. Materials and methods

2.1 Preparation of new biocarriers and media specifications

The equipment required for the preparation of the new biocarriers was a ZR4-6 six-way mixer which was stirred by the impellers of the stirring device to help the zeolite powders enter the polyurethane sponges. The detailed procedures and results are noted in the Supplementary Material. Before being added to the glass container, the polyurethane sponges were dried at 60 °C in an oven for 2h, then the resulting weight was recorded as m_1 . At the end of each running speed, it was necessary to take out the combined new biocarriers from the six-way mixer, then put it in the oven at 60 °C to dry for 12h. The weights named m_{2-1} , the m_{2-2} , the m_{2-3} , the m_{2-4} , and m_{2-5} m_{2-6} , respectively. Therefore, the value of $m_2 - m_1$ was the weight of the zeolite powders adsorbed by polyurethane sponges. Each condition was run three times to take the average, and finally the optimum speed and best combination time

were determined.

Sponges with a density of 28 kg/m^3 with 90 cells per 25 mm were purchased from Joyce Foam Pty, Australia. The polyurethane sponge biocarriers were cut into pieces with a diameter of $15 \times 15 \times 15 \text{ mm}$ and the specific surface area of a sponge cube was $0.846 \text{ m}^2/\text{g}$. The zeolite powders (purchased from Henan, China) were mainly composed of SiO_2 and contained a small amount of chemical elements such as Ca, Mg and Al. The particle size of zeolite powders was 100 mesh (0.15mm - more than 95% passing), the specific gravity was $2.1\text{--}2.6 \text{ g/cm}^3$ and the specific surface area was $23.4 \text{ m}^2/\text{g}$. After this preparation, the size of the new biocarriers remained consistent with that of the sponge biocarriers, but the density was 32 kg/m^3 .

2.2 Synthetic wastewater

The experiments were carried out with synthetic wastewater, which consisted of the following compounds: 110–120 mg/L total organic carbon (TOC), 28–33 mg/L $\text{NH}_4^+\text{-N}$, 2.7–3.5 mg/L total phosphorus, 0.5–2.5 mg/L $\text{NO}_3^-\text{-N}$ and 0.02–0.11 mg/L $\text{NO}_2^-\text{-N}$. The trace nutrient solution contained the following (mg/L): $\text{MgSO}_4 \cdot 7\text{H}_2\text{O}$, 5.07; $\text{CaCl}_2 \cdot 2\text{H}_2\text{O}$, 0.368; $\text{MnCl}_2 \cdot 7\text{H}_2\text{O}$, 0.275; $\text{ZnSO}_4 \cdot 7\text{H}_2\text{O}$, 0.44; $\text{CoCl}_2 \cdot 6\text{H}_2\text{O}$, 0.42; $\text{CuSO}_4 \cdot 5\text{H}_2\text{O}$, 0.391; FeCl_3 , 1.45; $\text{Na}_2\text{MoO}_4 \cdot 2\text{H}_2\text{O}$, 1.26; and yeast extract, 30 (Zhang et al., 2017). Based on the component of the synthetic wastewater, the TOC/TN (C/N) ratio of the influent in the experiments was around 3.5.

2.3 Experimental set-up and operation

Two rectangle-shaped MBBR reactors with a working volume of 12L were operating continuously in parallel under aerobic conditions for a period of 90 days, and both reactors

were filled with biocarriers with a filling percentage of 10%. Sponges with a density of 28 kg/m³ with 90 cells per 25 mm were purchased from Joyce Foam Pty, Australia. The activated sludge was collected from a secondary sedimentation tank at a local municipal wastewater treatment plant in Tianjin, China. The initial mixed liquor suspended solids (MLSS) was 2.8 g/L. The MBBR with fresh zeolite powder-based polyurethane sponge biocarriers (Z-MBBR) and the MBBR with fresh polyurethane sponge biocarriers (S-MBBR) were acclimatized for 15 days before operating in continuous mode at the flow rate of 16.7 mL/min, corresponding to a hydraulic retention time (HRT) of 12 h. Air was diffused in order to supply oxygen to the microbial mass for biological activity and to mix the biocarriers. The air flow was kept at around 0.09 m³/h in both MBBR reactors, and in this case the DO concentration ranged from 5.0-6.5mg/L. The pH was maintained at around 7.0 by adjusting it with NaCO₃ or H₂SO₄. Simultaneously, the reactors were both operated at room temperature (20±1 °C).

2.4 Analytic methods

TOC was measured using a TOC analyzer (TOC-VWP, Shimadzu, Japan). Other indexes for water quality, including NH₄⁺-N, NO₂⁻-N, NO₃⁻-N, MLSS and the mixed liquor volatile solids (MLVSS) are measured according to the standard methods (APHA et al., 2005).

Attached-growth biomass (AGBS) and volatile attached-growth biomass (VAGBS) in each of the biocarriers were obtained according the method reported in Zhang et al. (2016). Total nitrogen removal efficiency and simultaneous nitrification and denitrification (SND) were also calculated according to the study by Zhang et al. (2016):

$$\text{TN removal efficiency} = \left(1 - \frac{NH_4^+{}_{eff} + NO_2^-{}_{eff} + NO_3^-{}_{eff}}{NH_4^+{}_{inf} + NO_2^-{}_{inf} + NO_3^-{}_{inf}}\right) \times 100\% \quad (1)$$

$$SND = \left(1 - \frac{NO_2^-_{eff} + NO_3^-_{eff} - NO_2^-_{inf} - NO_3^-_{inf}}{NH_4^+_{inf} - NH_4^+_{eff}}\right) \times 100\% \quad (2)$$

where $NH_4^+_{inf}$, $NO_2^-_{inf}$ and $NO_3^-_{inf}$ are the NH_4^+ , NO_2^- and NO_3^- concentrations in the influent (mg/L), $NH_4^+_{eff}$, $NO_2^-_{eff}$ and $NO_3^-_{eff}$ are the NH_4^+ , NO_2^- and NO_3^- concentrations in the effluent (mg/L).

$$AGBS = \frac{m_b - m_a}{m_c} \quad (3)$$

$$VAGBS = \frac{m_b - m_d}{m_c} \quad (4)$$

where m_a is the weight of filter membrane dried at 105°C , m_b is the sum of the weight of filter membrane and microorganism from a carrier dried at 105°C , m_c is the weight of the carrier after removal of microorganisms dried at 105°C , m_d is the sum of the weight of filter membrane and microorganism from a carrier dried at 600°C .

2.5 Microelectrode preparation and microprofile measurements

The Unisense Microelectrode System (PA2000, Unisense, Denmark) was used to measure the DO and redox potential (ORP) on the 15th, 35th, 55th and 75th days. The DO and ORP of biocarriers were measured following the methods used as described previously (Cao et al., 2016) and an adjustment was made. When a biocarrier was removed from the reactor, the water in this reactor was removed as well and placed into the 250ml beaker. Here the wastewater was just submerged into the biocarrier to maintain the same environment as done in the reactor. Leveling with the surface of the water, the DO probe stopped after moving $5000\mu\text{m}$ inside the biocarrier. The step size of each profile was set to $100\mu\text{m}$ by the software (SensorTrace PRO V3.1.3, Unisense, Denmark). The measurement time for each point was 1s and the waiting time was 4s. In addition to measuring the depth, this changed to

7500 μm , with the ORPs being consistent with the measurement of DO. In order to ensure the accuracy of the data, three pieces of biocarriers were repeated in each reactor.

2.6 Microbial community analysis

The biofilm samples were collected from both reactors at different stages (15, 35, 55 and 75 days) to reveal microbial characteristics via high-throughput sequencing. The primer system (341F and 805R) can effectively amplify multiple variable regions (V3, V4) of 16S rDNA and accurately identify several species. After the extraction and quality inspection of the sample's genome DNA, the PCR amplification and product purification were carried out, and the Illumina MiSeq sequencing was lastly implemented. The indexes for calculating the community richness include ACE, Chao, Shannon, Simpson and so on, all of which were calculated by Mothur software.

3. Results and discussion

3.1 The performance of S-MBBR and Z-MBBR

Fig. 1 summarizes the removal efficiencies of TOC, $\text{NH}_4^+\text{-N}$, TN and SND in S-MBBR and Z-MBBR during the operation period. As shown in Fig. 1(a) and (b), both MBBR reactors removed more than 94% TOC and 97% $\text{NH}_4^+\text{-N}$ regardless of the type of biocarrier. Due to the existence of a large number of heterotrophic bacteria on the surface of biocarriers and bulk solution, a high removal rate of TOC can be achieved even if the number of anoxic/anaerobic bacteria was relatively low when the operation began. The biofilms on the biocarriers' surface was fully exposed to the bulk solution in the reactors, being in contact with a large amount of dissolved oxygen, thus this ammoniation and nitrification were so adequate that the $\text{NH}_4^+\text{-N}$

concentration rapidly decreased .

Although both MBBR reactors had almost the same TOC and $\text{NH}_4^+\text{-N}$ removal efficiencies at the HRT of 12 h and aeration flow of $0.09 \text{ m}^3/\text{h}$, the TN and SND conditions were very different. Based on Fig. 1(c), the efficiencies of TN on average in S-MBBR and Z-MBBR were $75.1 \pm 6.8\%$ and $84.2 \pm 4.8\%$, respectively. Correspondingly, the Z-MBBR performed better for SND ($90.7 \pm 4.1\%$), while $81.7 \pm 6.5\%$ of SND was obtained in the S-MBBR. The efficiency in removing $\text{NH}_4^+\text{-N}$ in the two MBBR reactors was basically the same, so the difference between the S-MBBR and Z-MBBR in terms of TN and SND is mainly in the denitrification process. This suggests that the denitrification capacity was the controlling factor that affected the MBBR system's ability to remove nitrogen (Tan et al., 2017).

By contrast, more denitrifying bacteria attached to the interior of the new zeolite powder which modified the polyurethane sponges. It is possible that this phenomenon may have the following explanations. Firstly, zeolite powders can enter the space of polyurethane sponges by physical rotation, making full use of the porosity and improving the specific surface area of the sponges, which is beneficial to the attachment of more denitrifying bacteria. The specific surface area of the polyurethane sponges and zeolite powders used in this study was $0.846 \text{ m}^2/\text{g}$ and $23.4 \text{ m}^2/\text{g}$, respectively so as the specific surface area of zeolite powders is much larger than that of polyurethane sponges. Therefore, when zeolite powders entered the pores and channels of the polyurethane sponges, the specific surface area of the whole biocarrier can be increased, reducing the pore size of the sponges to result in blocking the diffusion of oxygen to a certain extent. Because of the decrease of dissolved oxygen, the

denitrifying bacteria growing anoxia will gradually increase. Secondly, the occurrence of SND is due to the restriction of oxygen diffusion that causes the DO gradient in the biocarriers. As larger biomass attaches to the new zeolite powder-modified polyurethane sponges, the microbial metabolism consumes oxygen and then increases the oxygen concentration gradient. Therefore, the external contact of the biocarriers produces an ammonia and nitrification reaction. Meanwhile the internal oxygen is very rare and the denitrification reaction occurs, resulting in the removal of TN and SND increasing by $9.1 \pm 2.0\%$ and $9.0 \pm 2.4\%$, respectively.

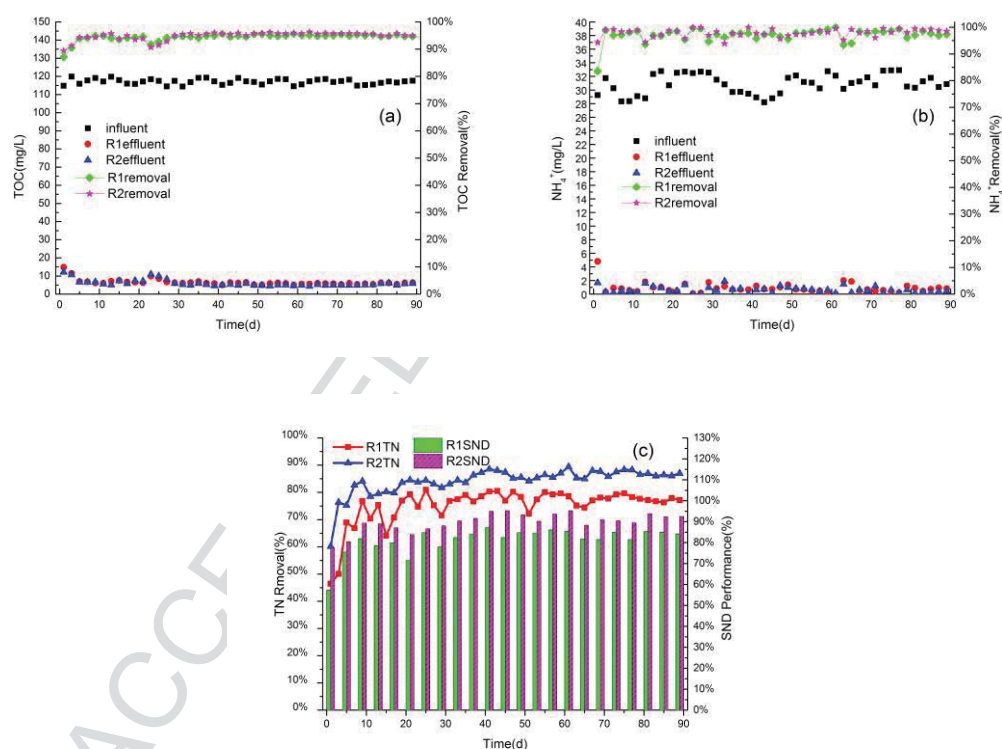


Fig. 1 Variations of TOC, NH₄⁺-N, TN concentrations and their removal efficiencies as well as SND performance in S-MBBR (R1) and Z-MBBR (R2): (a) TOC, (b) NH₄⁺-N, and (c) TN and SND

3.2 Formation and growth of the biofilm on the biocarriers

Due to the porous structure of polyurethane sponges, microorganisms constantly attach to the inner space of the biocarriers during the cultivation of biofilm (Chu and Wang, 2011; Luo et al., 2014). As the weight of biofilm on the biocarriers increases, so does the thickness of the biofilm. The increase of biofilm thickness is conducive to the formation of an anoxic environment in biocarriers (Guo et al., 2010), which promotes the process of SND and the removal of TN.

The sludge inoculated in the reactor was basically discharged on the 5th day, thus the biomass on biocarriers was the main factor affecting the whole reaction. From the obtained results shown in Table 1, whether it be the suspended biomass (MLSS) in bulk solution or the attached biomass (AGBS) on the biocarriers, it was obvious that Z-MBBR was better than S-MBBR. In particular, the amount of biofilm attached to the new biocarriers was 1.3 times more than that to the sponge carriers (0.470 ± 0.131 g/g carrier in the former, compared to 0.355 ± 0.099 g/g carrier in the latter). Previously, Zhang et al. (2017) studied the biomass of different filling rate with traditional polyurethane sponges as biocarriers. When the filling rate was 10%, the biomass was about 0.29g/g carrier, which was similar to that in S-MBBR, but less than that in Z-MBBR. After the inoculated sludge was discharged completely, the suspended biomass was mainly derived from the loss of biofilm on the biocarriers. In contrast, the phenomenon that the Z-MBBR had more suspended biomass showed that the metabolic rate in the new zeolite powder-modified polyurethane sponges was faster than the conventional sponge carriers. This led to a greater consumption of oxygen which improved the oxygen concentration gradient in the new zeolite powder-modified polyurethane sponge

carriers.

The growth rates of attached biofilm in the two MBBR reactors are described in Fig. 2. The whole process is divided into four stages, these being: discharge sludge (stage I: 0-10 days), rapid biofilm growth (stage II: 10-45 days), slow biofilm growth (stage III: 45-60 days) and biofilm maturation (stage IV: 60-90 days). During stage I, the unstable sludge attached to the surface of the biocarriers was discharged with the flow of water, while the growth rate of the biofilm was slow at this stage, leading to the downward trend of biomass. During stage II, the microorganisms grew rapidly in both MBBR reactors, and the growth rates of biofilm in S-MBBR and Z-MBBR were 0.0065 g/(carrier d) and 0.0095 g/(carrier d), respectively. During stages III and IV, the biofilm grew slowly to maturity. Throughout this process, S-MBBR revealed the average value of volatile attached-growth biomass was 0.279 ± 0.092 g aVAGBS/carrier, corresponding to 0.385 ± 0.119 g aVAGBS/carrier in Z-MBBR.

Table 1

MLSS, MLVSS, AGBS and VAGBS in the S-MBBR and Z-MBBR (mean data).

	MLSS(g/L)	MLVSS(g/L)	AGBS(g/g carrier)	VAGBS(g/g carrier)
S-MBBR	0.256±0.100	0.206±0.058	0.355±0.099	0.279±0.092
Z-MBBR	0.324±0.134	0.271±0.093	0.470±0.131	0.385±0.119

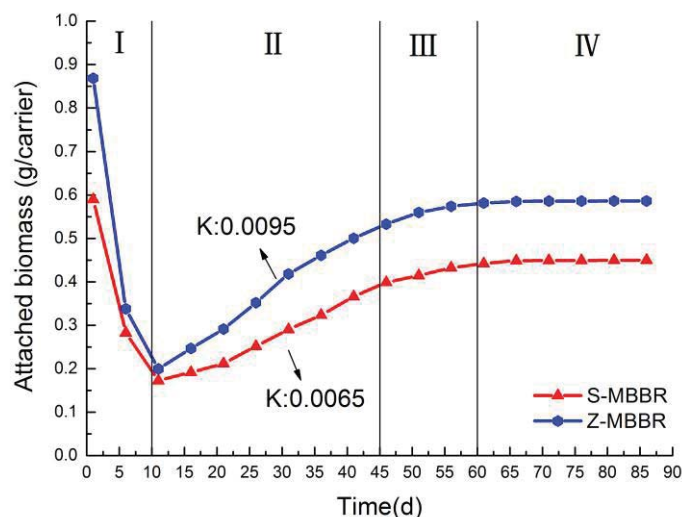


Fig. 2 Growth curve of the biofilm biomass in S-MBBR and Z-MBBR during the whole period.

3.3 DO and ORP profiles in biocarriers

3.3.1 DO profile within the biofilm

The DO concentration gradient in biofilm causing aerobic and anoxic areas is the key to successful simultaneous nitrification and denitrification. Controlling DO simultaneously can form aerobic and anoxic areas in different parts of the biofilm. This helps to influence the habitat and biodiversity of microorganisms within biocarriers (Tang et al., 2017b).

The DO concentration profiles within the biofilm of the two MBBR reactors at different stages are plotted in Fig. 3. The DO concentration in S-MBBR was around 2.1mg/L when the dissolved oxygen probe reached 5000 μ m from the biocarrier on the 15th day, whilst that in Z-MBBR was around 1.7mg/L (see Fig. 3(a)). Although difference at the same position within the two types of biocarriers, the concentration of dissolved oxygen was not reduced to zero. Since at this stage for all biocarriers, due to less biomass less dissolved oxygen consumed by

microbial respiration led to excessive oxygen entering the biocarriers. This resulted in the slow growth of denitrifying bacteria. The zeolite powder-based polyurethane sponges had more biomass, thus the internal oxygen of the new biocarriers was less than the sponge carriers. By the time when the two MBBR reactors were run for the 35th day (Fig. 3 (b)), the concentration of dissolved oxygen within the zeolite powder-based polyurethane sponges at 5000 μm was almost zero in Z-MBBR, and the DO within biocarriers in S-MBBR also fell below 1.0mg/L at the same position. This is in accordance with biomass growth in Fig. 2, which demonstrates that the biomass on the two types of carriers significantly increased.

From Fig. 3 (c), the concentration of dissolved oxygen dropped to zero when the probe traveled to around 4300 μm within the sponge carriers for the S-MBBR reactor on the 55th day. Hence, the concentration of dissolved oxygen had been zero at around 3800 μm inside the new biocarriers for the Z-MBBR reactor. This phenomenon showed that, on the one hand, the consumption of oxygen quickened when the biomass increased in all biocarriers. There was great space contact in the biocarriers, and low oxygen is suitable for the growth of denitrifying bacteria. On the other hand, it was shown that the biomass of the new biocarriers was obviously higher than that of the traditional biocarriers. Therefore, the total nitrogen removal rate and the SND performance were superior in Z-MBBR. As the oxygen concentration decreased in biocarriers, the space for the growth of the denitrifying bacteria in the two types of biocarriers increased in the last stage (Fig. 3(d)), which can ensure stable and efficient simultaneous nitrification and denitrification. Although the concentration of dissolved oxygen inside the biocarriers was smaller in the middle and later operation stages, there was also a large number of nitrifying bacteria in the liquid of reactors or on the surface

of biocarriers. Consequently, the nitrification process could proceed smoothly.

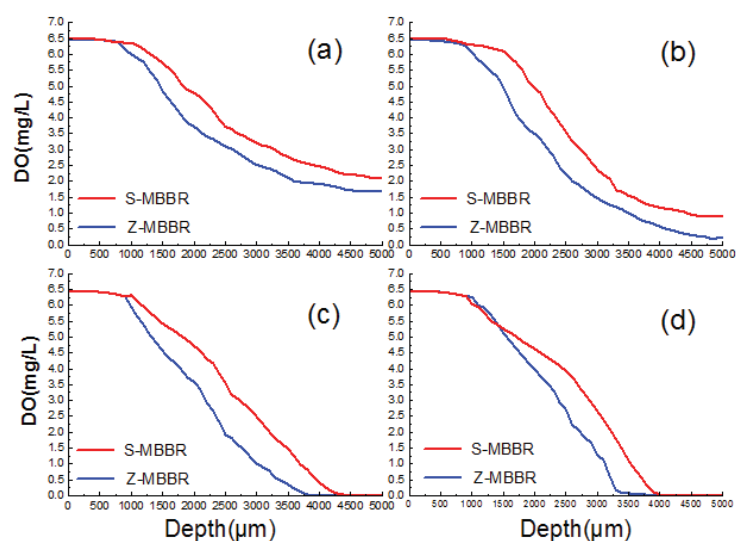


Fig. 3 DO profile within the biofilm at different time points: (a) 15 days; (b) 35 days; (c) 55 days; (d) 75 days.

3.3.2 Redox potential profile within the biofilm

Redox reaction plays a key role in the existence and migration of various organic and inorganic species. Nitrification is the process of improving the nitrogen element valence, which belongs to the oxidation reaction. Conversely, the denitrification reduced nitrogen valence is part of the reduction reaction. Because of the SND in biocarriers, oxidation reaction and reduction reaction occur at the same time during the process of nitrogen removal, so does the acidity and alkalinity. Therefore, determination of ORP can directly reflect the state of nitrification and denitrification occurring in the biofilm.

The ORP profiles within biocarriers of the two MBBR reactors at different stages are illustrated in Fig. 4. As shown in Fig. 4(a), the ORP decreased from 419mV to 87mV from the surface to the center of the sponge carriers in the S-MBBR reactor. Correspondingly, the ORP

in new biocarriers in the Z-MBBR reactor dropped from 422mV to 61mV. There was little difference in ORP between the two types of biocarriers at this stage. However, at the center of the biocarriers, the ORP of the zeolite powder-based polyurethane sponges was relatively low, indicating that more denitrification occurred inside the new biocarrier. Due to the fact that the ORP in both biocarriers was greater than 60mV, the nitrification reaction was dominant in the two MBBR reactors on the 15th day. When the two MBBR reactors were run to the 35th day (Fig. 4(b)), the ORP at the centre of the sponge carriers and the new biocarriers was 55mV and 39mV, respectively. With the continuous growth of biofilm occurring in the biocarriers, the aerobic microorganisms grew and consumed some of the dissolved oxygen. Therefore the ratio of denitrifying bacteria increased with the reduction of oxygen in biocarriers. As depicted in Fig. 4 (c), the ORP of the sponge carriers and the new biocarriers decreased to 36mV and 16mV, respectively, due to strengthening of the denitrification reaction. At the last stage (see Fig.4 (d)), the minimum ORP of the center of the sponge carriers reached 25mV, and that of the new biocarriers had reached 9mV. According to another study (Won & Ra, 2011), SND should proceed smoothly when the ORP is less than $>30\text{mV}$, as in accordance with the phenomena shown in Fig. 1 (c).

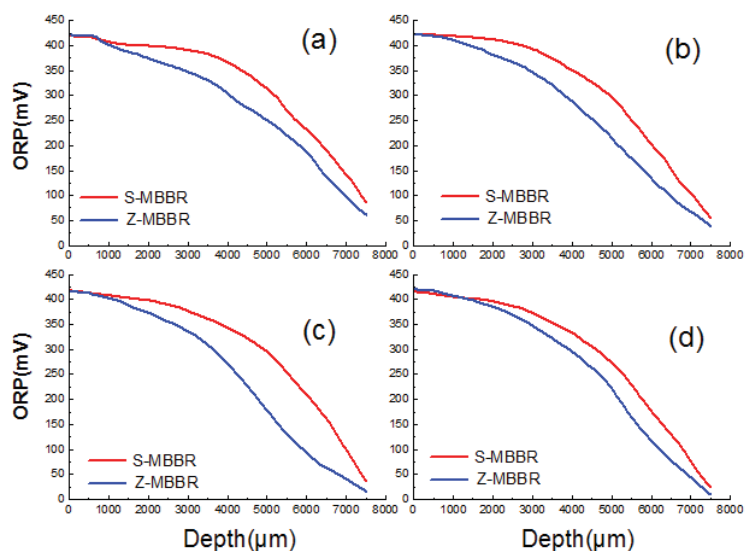


Fig. 4 ORP profile within the biofilm at different time points: (a) 15 days; (b) 35 days; (c) 55 days; (d) 75 days.

In general, the denitrification effect in Z-MBBR was stronger than that of S-MBBR during the whole process of the two reactors. This is due to the zeolite powders were able to enter the pores and channels of the polyurethane sponges, making full use of their porous properties. This could improve the specific surface area of the new biocarriers and be beneficial to the attachment of more microorganisms. The metabolism of microorganisms on the new biocarriers consumed a large amount of dissolved oxygen, thus creating a good denitrification environment and accelerating the simultaneous nitrification and denitrification process of Z-MBBR.

3.4 Microbial community analysis

3.4.1 Biodiversity analysis

Microbial communities in biocarriers are the main factors affecting the performance of the reactors (Liu et al., 2018; Tang et al., 2017a). However, the different biocarriers used will

lead to a change in the microbial diversity. The species richness and diversity indices including sequence number, OTU number, ACE, Chao1, Shannon, Simpson and so on are summarized in Table 2. From Table 2, the inoculated sludge had 61117 sequences and 1594 OTUs. By contrast, the sequence number of biofilm samples in the S-MBBR was 55874-67087, while that in the Z-MBBR was 57332-72310. The biological diversity in the two MBBR reactors both display the tendency to increase first and then decrease, reaching a maximum value on the 55th day. The Shannon index is often used to estimate microbial diversity in samples, and the results showed that the biodiversity in the Z-MBBR was more volatile and higher in the later than S-MBBR. ACE and Chao1 are commonly used to assess the total number of species. In the latter period for the two reactors (75th day), the ACE and Chao1 indices of the biofilm samples within the Z-MBBR reactor were 833 and 923, respectively. Correspondingly, they were 566 and 553 in the S-MBBR reactor meaning that the application of the zeolite powder-based polyurethane sponges increased the total number of species in the reactor. In addition, the Good's Coverage in the two MBBR reactors did not differ greatly throughout the whole operation.

Table 2

Biodiversity evaluation of both MBBR reactors at different time points: inoculated sludge (D1); the samples of S-MBBR at 15, 35,55 and 75days (D15A, D35A, D55A and D75A); the samples of Z-MBBR at 15, 35,55 and 75days (D15B, D35B, D55B and D75B).

Sample	Sequence number	OTU number	Shannon index	ACE index	Chao1 index	Coverage	Simpson
D ₁	61117	1594	8.827	8767.725	9184.585	0.954	0.993
D _{15A}	55874	6816	5.691	825.508	843.526	0.996	0.948
D _{15B}	63974	5290	5.975	890.864	855.031	0.996	0.96
D _{35A}	64315	4567	6.187	820.983	853.016	0.996	0.966
D _{35B}	71798	10042	5.367	814.585	773.725	0.996	0.902
D _{55A}	67087	7272	5.953	827.873	865.231	0.996	0.952
D _{55B}	72310	14708	5.254	755.544	754.08	0.997	0.882
D _{75A}	62622	19534	4.442	566.242	553.902	0.998	0.81
D _{75B}	57332	15601	5.517	883.976	923.623	0.996	0.876

The differences and similarities among the inoculated sludge and biofilm samples were revealed through the Principal Coordinate Analysis (PCoA) method. The weighted UniFrac distance between the sample points represents how the microbial communities in the samples are similar. The closer the distance is, the higher the similarity is. Sample D1 was the original sludge inoculated into the S-MBBR and Z-MBBR. The microbial communities in all biofilm samples were very different from that in the inoculated sludge. This may be the microorganisms whose generation time is long prefer to grow on the biocarriers, which leads

to a long food chain of biofilms, and the abundance of bacteria on biofilms is far higher than that in the activated sludge. During the first 15 days of the experiment, there was only a slight difference in the microbial communities between the two samples (D15A and D15B). From the test results for the 35th day and 55th day, a certain difference emerged in the microbial communities between the S-MBBR and Z-MBBR, and this difference decreased again on the 75th day (D75A and D75B). From the perspective of the two MBBR reactors' running time, the variety of species richness was the greatest in the early stage (15-35), followed by the middle stage (35-55 days), and the difference was the smallest in the latter stage (55-75 days). This indicated that the microbial communities' stability improved with the continuous maturation of biofilms on the biocarriers, and was consistent with the reactors' removal efficiency. Although there was a difference in species richness among different biofilm samples, the highest abundant organisms in all the biofilm samples were similar (Young et al., 2017).

3.4.2 Microbial community evolution of biofilms

A total of 29 phyla and 48 classes were identified from the inoculated sludge and eight biofilm samples of the two MBBR reactors. At the phylum level (Fig. 5(a)), *Proteobacteria* and *Bacteroidetes* were the two most dominant bacteria during the whole process involving the two MBBR reactors, which is found in most other studies (Wang et al., 2018a; Wang et al., 2018b). Both the *Proteobacteria* and *Bacteroidetes* belong to the Gram-negative bacteria, and their surface is mainly composed of lipopolysaccharides (Atabek & Camesano, 2007), which enables them to attach easily to the surface of the biocarriers. For the S-MBBR samples, *Proteobacteria* decreased continuously during the first 15 days, increased to 55.36% and then

eventually stabilized (D1: 57.78%, D15A: 38.36%, D35A: 55.36%, D55A: 55.34%, D75A: 54.71%), while the *Bacteroidetes* showed the opposite trend (D1: 19.96%, D15A: 51.71%, D35A: 36.07%, D55A: 25.44%, D75A: 26.69%). For the samples of Z-MBBR, *Proteobacteria* decreased continuously during the first 15 days, then increased to 67.91% from the 15th day to the 75th day (D1: 57.78%, D15B: 26.87%, D35B: 41.52%, D55B: 65.55%, D75B: 67.91%), while the *Bacteroidetes* did the opposite (D1: 19.96%, D15B: 59.91%, D35B: 45.62%, D55B: 21.12%, D75B: 12.11%). Compared with the inoculated sludge, *Saccharibacteria* increased during the early operational stage (1~35d), and decreased in the later stage (35~75d) in both MBBR reactors, with the highest ratio of *Saccharibacteria* in the S-MBBR recording 7.51%, and the corresponding 11.48% in Z-MBBR.

In comparison to the inoculated sludge, the ratio of *Verrucomicrobia* suddenly increased (from 1.82% to 11.07%) in the S-MBBR from the 15th day to the 35th day, and in the Z-MBBR, *Verrucomicrobia* increased from 0.20% to 8.82% gradually throughout the whole operation. The microbial shift is most likely due to the *Verrucomicrobia* belonging to the denitrification communities (Lu et al., 2014), and the DO in biocarriers gradually decreased in the middle and later stages of the two MBBR reactors. This created superior conditions for the survival of the *Verrucomicrobia*. Additionally, *Acidobacteria* was one of the third dominant bacteria in the inoculated sludge, but it had a relatively small proportion in the two MBBR reactors, which may result from the fact that *Acidobacteria* does not adapt to the growth environment provided by the biofilm.

At the class level (Fig. A3), *Betaproteobacteria*, *Gammaproteobacteria*, *Alphaproteobacteria* and *Deltaproteobacteria* were the four most abundant classes in

Proteobacteria, which took up 26.90%~67.92% of the total microbes. In addition, the class *Betaproteobacteria* contained the highest population of the *Proteobacteria* in most of the samples, especially the proportions of *Betaproteobacteria* in D75A and D75B which were 43.89% and 43.05%, respectively. *Betaproteobacteria*, the contained *Nitrosococcus oceanus* and *Rhodocyclus* have a close relationship with the removal of nitrogen (Tang et al., 2017a), and this plays an important role in the normal and efficient operation of biofilms.

Sphingobacteriia, which are major microorganisms involved in the removal of COD and nitrogen (Tang et al., 2017a), constituted the largest population of *Bacteroidetes* (average amounts in the S-MBBR and Z-MBBR were 16.33% and 18.70%, respectively), followed by the *Flavobacteriia* (average amounts in the S-MBBR and Z-MBBR were 7.63% and 2.37%, respectively), and *Bacilli* (average amounts in the S-MBBR and Z-MBBR were 0.72% and 0.46%, respectively). From Fig. A3, the proportion of *Cytophagia* in inoculated sludge was relatively small, but it increased gradually when the biofilm grew on biocarriers and became one of the main dominant bacteria. For example, in D55A and D35B the proportions of *Cytophagia* were 14.34% and 25.96%, respectively). This indicated that *Cytophagia* had prominent viscosity and was suitable for growing on biofilms. It can also be speculated that this class may secrete viscous substances and promote the formation of biofilm.

Greater differences were observed among the samples from inoculated sludge and biofilms at the genus level. The abundant genera in inoculated sludge, such as *Terrimonas*, *Ferribacterium* and *Thauera*, were specific to the activated sludge and seldom found in the biofilm samples. In recent years the genus *Terrimonas* has become a newly established genus; it is a rod-shaped Gram-negative bacteria (Jiang et al., 2018) and belongs to *Sphingobacteriia*.

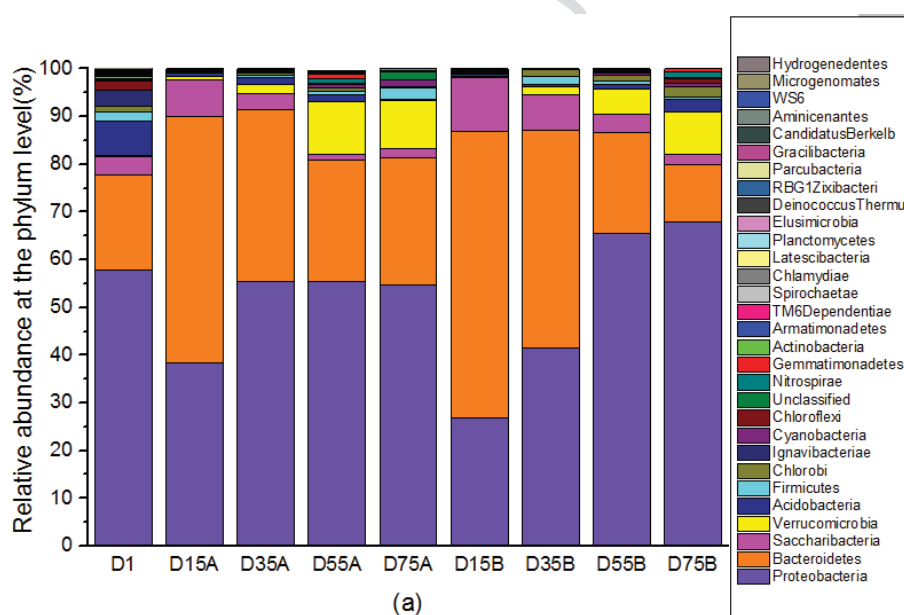
In addition, *Ferruginibacter* is commonly shared by activated sludge samples and capable of hydrolyzing organic matter (Han et al., 2015). As in the biofilm samples, the microbial communities between the S-MBBR and Z-MBBR could be differentiated. However, the five most abundant microorganisms among all the samples were basically the same, namely, *Sphaerotilus*, *Thermomonas*, *Flavobacterium*, *Prostheco bacter* and *Enterobacter*.

From Fig. 5(b), an interesting phenomenon is evident in that a very small proportion of the genus *Thermomonas* existed in the inoculated sludge. However, this changed greatly when the two MBBR reactors were operating. In the early stage there was a significant increase in the genus *Thermomonas* in the S-MBBR, but gradually reduced to a very small proportion in the later stage (D15A: 16.10%, D35A: 8.62%, D55A: 0.49%, D75A: 0.12%). The same thing happened in the Z-MBBR (D15B: 14.86%, D35B: 2.71%, D55B: 1.08%, D75B: 0.89%). *Thermomonas*, a kind of Gram-negative bacteria, usually occurs in filaments (Busse et al., 2002), which can utilize organic electron donors and reduce nitrate or nitrite to molecular nitrogen (Han et al., 2015).

Another interesting phenomenon concerns the genus *Sphaerotilus*. It was not detected in the inoculated sludge, but it became the dominant bacteria when the experiment lasted to the 35th day (e.g. in D35A and D35B, the ratios of *Sphaerotilus* were 10.85% and 22.35%, respectively) and retained the highest proportion when the experiment ended. The genus *Sphaerotilus* is a chemoheterotrophic Gram-negative bacteria. Although it is strictly aerobic, it can grow well under low oxygen pressure. Therefore, it is inferred that the concentration of dissolved oxygen (Fig. 3) within biocarriers was suitable for the survival of *Sphaerotilus* on the 35th day. As the concentration of dissolved oxygen in biocarriers had been consumed, the

proportion of the population gradually increased.

Due to the diversity of microbial species attached to the biofilms, it is difficult to accurately describe the changes in each microorganism at the genus level. *Flavobacterium* is in charge of denitrification under heterotrophic conditions (Huang et al., 2015), and the average proportions were 1.47% and 5.57% in the S-MBBR and Z-MBBR, respectively. This was consistent with the Z-MBBR demonstrating the better denitrification than the S-MBBR. *Prostheco bacter* and *Enterobacter* are both chemoheterotrophic microorganisms, and they play an important role in removing organic matter. Furthermore the populations on biocarriers will change when different types of carbon source are added (Lu et al., 2014).



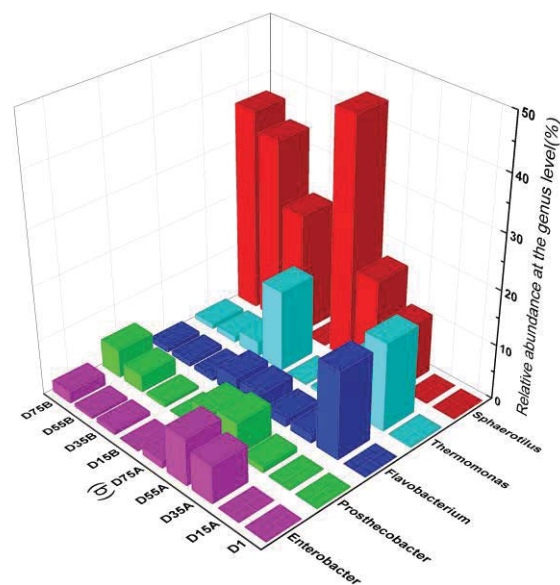


Fig. 5. Microbial composition: (a) Relative abundance at the phylum level; (b) Relative abundance of the maximum genus contained in each sample. Inoculated sludge (D1); the samples of S-MBBR at 15, 35,55 and 75days (D15A, D35A, D55A and D75A); the samples of Z-MBBR at 15, 35,55 and 75days (D15B, D35B, D55B and D75B).

3.4.3 The functional genera on nitrogen removal

Biological nitrogen removal consists of two processes: nitrification and denitrification. The former is the conversion of ammonia nitrogen into nitrite under the action of ammonia oxidizing bacteria (AOB), and then it is converted into nitrate by the action of nitrite oxidizing bacteria (NOB). The latter transforms nitrate into molecular nitrogen by nitrite under the action of denitrifying bacteria (DNB). In general, *Nitrosomonas* is the most common genus in AOB, and *Nitrospira* is the most common genus in NOB (Young et al., 2017; Zhao et al., 2015). Although denitrifying bacteria has not yet been strictly defined according to previous studies, *Thermomonas*, *Dechloromonas*, *Thauera*, *Zoogloea*, *Brevundimonas*, *Klebsiella* and *Flavobacterium* have the ability to reduce nitrate or nitrite into molecular nitrogen (Han et al., 2015; Lu et al., 2014; Tang et al., 2017a) . The relative

abundance of AOB, NOB and DNB in both inoculated sludge and biofilm samples are shown in Fig. 6. The proportion of AOB in all samples was about 0.65%, showing no significant difference (Fig. 6 (a)). Therefore, there was no difference in the removal of $\text{NH}_4^+\text{-N}$ between Z-MBBR and S-MBBR. Both exhibited high removal efficiencies of 97% $\text{NH}_4^+\text{-N}$ on average throughout the process.

In addition to the relatively small amount of NOB in the inoculated sludge, the content of NOB in other biofilm samples was about 0.25% (Fig. 6 (b)). There was no accumulation of nitrite despite the proportion of NOB being lower than that of AOB. This suggested that once NOB is accumulated, it will have enough capacity to transform nitrite into nitrate (Young et al., 2017). It also implied that denitrification is the rate limiting step of simultaneous nitrification and denitrification in MBBR. As shown in Fig. 6(c), the content of the DNB increased when the DO concentration in the biocarriers decreased ($\text{D75} > \text{D55} > \text{D35} > \text{D15}$). As well, the content of DNB in the Z-MBBR was higher than that in the S-MBBR at the same stage, which was consistent with the former's high TN removal efficiency and SND performance.

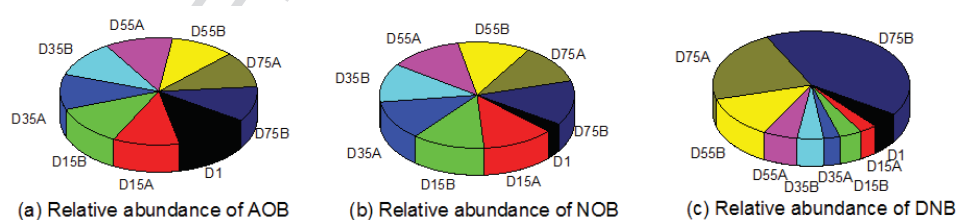


Fig. 6. Relative abundance of (a)AOB, (b)NOB and (c)DNB of all samples: inoculated sludge (D1); the samples of S-MBBR at 15, 35,55 and 75days (D15A, D35A, D55A and D75A); the samples of Z-MBBR at 15, 35,55 and 75days (D15B, D35B, D55B and D75B).

4. Conclusions

Comparative analysis indicated that there was no significant difference in TOC and $\text{NH}_4^+\text{-N}$ removal between the S-MBBR and Z-MBBR. However, the TN removal efficiency and SND performance in Z-MBBR were nearly 10% higher than those in S-MBBR. The distribution of DO and ORP inside the biocarriers was investigated, revealing a more suitable environment existed in the new biocarriers for denitrification. Additionally, the analysis of microbial communities demonstrated that not only microbial diversity but also the denitrifying bacteria were abundant in the Z-MBBR. In general, the new Z-MBBR can be a practical option for applying in a hybrid treatment to enhance nitrogen removal from wastewater.

Acknowledgements

This study was supported by the National Natural Science Foundation of China (Grant No. 51378338). The authors are also grateful for the support of Tianjin Chengjian University, School of Environmental and Municipal Engineering and University of Technology, Sydney, Centre for Technology in Water and Wastewater, School of Civil and Environmental Engineering.

Supplementary Information

Supplementary materials associated with this article can be found in the online version.

References

- Abzazou, T., Araujo, R.M., Auset, M., Salvadà³, H. 2016. Tracking and quantification of nitrifying bacteria in biofilm and mixed liquor of a partial nitrification MBBR pilot plant using fluorescence in situ hybridization. *Science of the Total Environment*, **541**, 1115-1123.
- APHA, AWWA, WEF, 2005. Standard Methods for the Examination of Water and Wastewater, 20th ed. American Public Health Association, Washington, D.C.
- Atabek, A., Camesano, T.A. 2007. Atomic force microscopy study of the effect of lipopolysaccharides and extracellular polymers on adhesion of *Pseudomonas aeruginosa*. *Journal of Bacteriology*, **189**(23), 8503-8509.
- Bakar, S.N.H.A., Hasan, H.A., Mohammad, A.W., Abdullah, S.R.S., Haan, T.Y., Ngteni, R., Yusof, K.M.M. 2018. A review of moving-bed biofilm reactor technology for palm oil mill effluent treatment. *Journal of Cleaner Production*, **171**(10), 1532-1545.
- Busse, H.J., Kämpfer, P., Moore, E.R., Nuutinen, J., Tsitko, I.V., Denner, E.B., Vauterin, L., Valens, M., Rosselló-Mora, R., Salkinoja-Salonen, M.S. 2002. *Thermomonas haemolytica* gen. nov., sp. nov., a gamma-proteobacterium from kaolin slurry. *International Journal of Systematic & Evolutionary Microbiology*, **52**(Pt 2), 473-483.
- Cao, Y., Zhang, C., Rong, H., Zheng, G., Zhao, L. 2016. The effect of dissolved oxygen concentration (DO) on oxygen diffusion and bacterial community structure in moving bed sequencing batch reactor (MBSBR). *Water Research*, **108**, 86-94.
- Chu, L., Wang, J. 2011. Nitrogen removal using biodegradable polymers as carbon source and biofilm carriers in a moving bed biofilm reactor. *Chemical Engineering Journal*, **170**(1),

220-225.

- Chu, L., Wang, J., Quan, F., Xing, X.H., Tang, L., Zhang, C. 2014. Modification of polyurethane foam carriers and application in a moving bed biofilm reactor. *Process Biochemistry*, **49**(11), 1979-1982.
- Deng, L., Guo, W., Ngo, H.H., Zhang, X., Wang, X.C., Zhang, Q., Chen, R. 2016. New functional biocarriers for enhancing the performance of a hybrid moving bed biofilm reactor-membrane bioreactor system. *Bioresource Technology*, **208**, 87-93.
- Gao, L., Zhou, W., Wu, S., He, S., Huang, J., Zhang, X. 2018. Nitrogen removal by thiosulfate-driven denitrification and plant uptake in enhanced floating treatment wetland. *Science of the Total Environment*, **621**, 1550-1558.
- Guo, W., Ngo, H.H., Dharmawan, F., Palmer, C.G. 2010. Roles of polyurethane foam in aerobic moving and fixed bed bioreactors. *Bioresource Technology*, **101**(5), 1435-1439.
- Han, X., Wang, Z., Ma, J., Zhu, C., Li, Y., Wu, Z. 2015. Membrane bioreactors fed with different COD/N ratio wastewater: impacts on microbial community, microbial products, and membrane fouling. *Environmental Science & Pollution Research International*, **22**(15), 11436-11445.
- Huang, C., Li, Z.L., Chen, F., Liu, Q., Zhao, Y.K., Zhou, J.Z., Wang, A.J. 2015. Microbial community structure and function in response to the shift of sulfide/nitrate loading ratio during the denitrifying sulfide removal process. *Bioresource Technology*, **197**(2), 227-234.
- Jiang, W.K., Lu, M.Y., Cui, M.D., Wang, X., Wang, H., Yang, Z.G., Zhu, S.J., Zhou, Y.D., Hu, G., Hong, Q. 2018. *Terrimonas soli* sp. nov., isolated from farmland soil. *International*

Journal of Systematic & Evolutionary Microbiology, **68**(3), 819-823.

Liu, Q., Yang, Y., Mei, X., Liu, B., Chen, C., Xing, D. 2018. Response of the microbial community structure of biofilms to ferric iron in microbial fuel cells. *Science of the Total Environment*, **631**, 695–701.

Lu, H., Chandran, K., Stensel, D. 2014. Microbial ecology of denitrification in biological wastewater treatment. *Water Research*, **64**(7), 237-254.

Luo, Y., Guo, W., Ngo, H.H., Long, D.N., Hai, F.I., Kang, J., Xia, S., Zhang, Z., Price, W.E. 2014. Removal and fate of micropollutants in a sponge-based moving bed bioreactor. *Bioresource Technology*, **159**(159), 311-319.

Mao, Y., Quan, X., Zhao, H., Zhang, Y., Chen, S., Liu, T., Quan, W. 2017. Accelerated startup of moving bed biofilm process with novel electrophilic suspended biofilm carriers. *Chemical Engineering Journal*, **315**, 364-372.

Odegaard, H., Rusten, B. 1994. A new moving bed biofilm reactor - application and results. *Water Science & Technology*, **29**, 157-165.

Peng, P., Huang, H., Ren, H., Ma, H., Lin, Y., Geng, J., Xu, K., Zhang, Y., Ding, L. 2018. Exogenous N-acyl homoserine lactones facilitate microbial adhesion of high ammonia nitrogen wastewater on biocarrier surfaces. *Science of the Total Environment*, **624**, 1013-1022.

Sancho, I., Licon, E., Valderrama, C., Arespachaga, N.D., López-Palau, S., Cortina, J.L. 2017. Recovery of ammonia from domestic wastewater effluents as liquid fertilizers by integration of natural zeolites and hollow fibre membrane contactors. *Science of the Total Environment*, **584–585**, 244-251.

- Sbardella, L., Fenu, A., Weemaes, M., Comas, J., Roda, I.R. 2018. Advanced biological activated carbon filter for pharmaceutical active compounds removal from treated wastewater. *Science of the Total Environment*, **636**, 519–529.
- Shi, Y., Huang, C., Gamal, E.M., Liu, Y. 2017. Optimization of moving bed biofilm reactors for oil sands process-affected water treatment: The effect of HRT and ammonia concentrations. *Science of the Total Environment*, **598**, 690-696.
- Tan, C., Xu, H., Cui, D., Zuo, J., Li, J., Ji, Y., Qiu, S., Yao, L., Chen, Y., Liu, Y. 2017. Effects of tourmaline on nitrogen removal performance and biofilm structures in the sequencing batch biofilm reactor. *Journal of Environmental Sciences*, **67**, 127-135.
- Tang, B., Chen, Q., Bin, L., Huang, S., Zhang, W., Fu, F., Li, P. 2017a. Insight into the microbial community and its succession of a coupling anaerobic-aerobic biofilm on semi-suspended bio-carriers. *Bioresource Technology*, **247**, 591-598.
- Tang, B., Song, H., Bin, L., Huang, S., Zhang, W., Fu, F., Zhao, Y., Chen, Q. 2017b. Determination of the profile of DO and its mass transferring coefficient in a biofilm reactor packed with semi-suspended bio-carriers. *Bioresource Technology*, **241**, 54-62.
- Walser, S.M., Brenner, B., Wunderlich, A., Tuschak, C., Huber, S., Kolb, S., Niessner, R., Seidel, M., Höller, C., Herr, C.E. 2016. Detection of Legionella-contaminated aerosols in the vicinity of a bio-trickling filter of a breeding sow facility - A pilot study. *Science of the Total Environment*, **575**, 1197-1202.
- Wang, L., Li, Y., Wang, L., Zhu, M., Zhu, X., Qian, C., Li, W. 2018a. Responses of biofilm microorganisms from moving bed biofilm reactor to antibiotics exposure: Protective role of extracellular polymeric substances. *Bioresource Technology*, **254**, 268-277.

- Wang, X., Bi, X., Hem, L.J., Ratnaweera, H. 2018b. Microbial community composition of a multi-stage moving bed biofilm reactor and its interaction with kinetic model parameters estimation. *Journal of Environmental Management*, **218**, 340-347.
- Won, S.G., Ra, C.S. 2011. Biological nitrogen removal with a real-time control strategy using moving slope changes of pH(mV)- and ORP-time profiles. *Water Research*, **45**(1), 171-178.
- Young, B., Banihashemi, B., Forrest, D., Kennedy, K., Stintzi, A., Delatolla, R. 2016. Meso and micro-scale response of post carbon removal nitrifying MBBR biofilm across carrier type and loading. *Water Research*, **91**, 235-243.
- Young, B., Delatolla, R., Kennedy, K., Laflamme, E., Stintzi, A. 2017. Low temperature MBBR nitrification: Microbiome analysis. *Water Research*, **111**, 224-233.
- Zhang, X., Chen, X., Zhang, C., Wen, H., Guo, W., Ngo, H.H. 2016. Effect of filling fraction on the performance of sponge-based moving bed biofilm reactor. *Bioresource Technology*, **219**, 762-767.
- Zhang, X., Song, Z., Guo, W., Lu, Y., Qi, L., Wen, H., Ngo, H.H. 2017. Behavior of nitrogen removal in an aerobic sponge based moving bed biofilm reactor. *Bioresource Technology*, **245**, 1282-1285.
- Zhao, Y., Fang, Y., Jin, Y., Huang, J., Ma, X., He, K., He, Z., Wang, F., Zhao, H. 2015. Microbial community and removal of nitrogen via the addition of a carrier in a pilot-scale duckweed-based wastewater treatment system. *Bioresource Technology*, **179**, 549-558.